

# Physicochemical and Morphological Evaluation of Potato Starch-Olive Oil Bio-Composite Films Incorporated with Graphene Oxide

**Farajpour, Romina**

*Department of Food Science and Technology, North Tehran Branch, Islamic Azad University, Tehran, I.R. IRAN*

**Emam Djomeh, Zahra<sup>\*+</sup>**

*Department of Food Science, Engineering and Technology, Faculty of Agricultural Engineering and Technology, University of Tehran, Karaj, I.R. IRAN*

**Ehsani, Morteza**

*Department of Polymer Processing, Iran Polymer and Petrochemical Institute, Tehran, I.R. IRAN*

**Moeini, Sohrab**

*Department of Food Science and Technology, North Tehran Branch, Islamic Azad University, Tehran, I.R. IRAN*

**Tavakolipour, Hamid**

*Department of Food Science and Technology, Sabzevar Branch, Islamic Azad University, Sabzevar, I.R. IRAN*

**Safaeian, Shila**

*Department of Food Science and Technology, North Tehran Branch, Islamic Azad University, Tehran, I.R. IRAN*

**ABSTRACT:** *The fabrication of potato starch-olive oil-graphene oxide bio-composite films was prepared via casting films-forming emulsion by adding Graphene Oxide (GO) to the Potato Starch-Olive Oil (PS/OO) matrix. The effects of olive oil and various amounts of graphene oxide on the performance of potato starch films were studied. Based on the results a combination of olive oil and GO was applied to diminish the Water Vapor Permeability (WVP) of the controlled films. Meantime, water solubility and moisture content decreased with olive oil incorporation and further decreased with increasing graphene oxide content. The addition of GO and olive oil into the films decreased the wettability of films. The mechanical strength was increased by the increment of GO and decreased*

---

*\*To whom correspondence should be addressed.*

*+ E-mail: emamj@ut.ac.ir*

*1021-9986/2023/8/2615-2628*

*14/\$/6.04*

*with olive oil incorporation. The color properties and UV transmittance of the neat film were affected by adding olive oil and GO. XRD proved that the GO layers were intercalated in the PS/OO emulsion structure and FT-IR demonstrated that new interactions were formed between PS/OO/GO. Scanning Electron Microscope (SEM) demonstrated the dispensation of GO sheets inside the emulsion network. The surface roughness of films increased by adding GO and olive oil. Dynamic mechanical tests revealed that the incorporation of GO improves the thermal resistance, and storage modulus of the films, and diminished with olive oil incorporation.*

**KEYWORDS:** *Potato starch; Olive oil; Graphene oxide; Bio-composite film.*

## INTRODUCTION

Past couple of decades, numerous investigations have been accomplished on toward the generation of bio-compatible and green polymers with natural origins, because they can be a viable solution for disposing of plastic packaging materials [1]. Biopolymers such as lipids, proteins, polysaccharides were considered to be renewable [2, 3]. In particular, starch, a natural polysaccharide, is inexpensive, biodegradable, and has been used for packaging utilizations [4]. Starch-based films represent appropriate physical characteristics, since they are colorless, odorless, tasteless and impermeable to oxygen [5]. However, it has some disadvantages, including moisture sensitivity, weak mechanical strength, high UV radiation transmission, and high brittleness [6]. To alleviate these problems, bio-composites are often modified by cross-linking agents or blended with other synthetic polymers, biopolymers, hydrophobic substances, or nanoreinforcements [7]. One approach to achieve a better water vapor barrier is incorporating the hydrophilic films with hydrophobic components like oil [8]. Olive oil is a vegetable oil which owing to its upper amount of oleic acid, has a liquid nature at environment temperature and makes it easy to mix with biopolymers. Olive oil was used to prepare films with better barrier properties and plasticized films for packaging. Using lipids into biodegradable films were caused a notable decrease in their mechanical strength, and thermal quality [9]. In recent years, the introduction of reinforcing fillers to enhance the physicochemical properties of biopolymers has received much attention and thus improves their functionality, processability, and end-use performance [3, 10, 11]. Among various types of fillers, Graphene Oxide (GO) has extensively been investigated owing to its enormous

potential for enhancing thermo-mechanical properties and shows large specific surface area [12]. GO has functional groups on the original sheets like phenol, -OH, epoxide and -COOH at its sides [13, 14]. This causes GO act as a hydrophilic-hydrophobic molecule (amphoteric) that can behave like a colloidal surfactant [15]. GO can be used in Pickering emulsions (no added electrolytes or surfactants) or emulsions [16]. In addition, GO has great potential in many applications, including electrical conductivity [17], energy storage devices, anti-static coating[18], and biomedical engineering sphere [1]. Furthermore, GO sheets possess superior thermal, mechanical and barrier properties [10, 19] and also exhibit high biocompatibility and antibacterial activity [20]. Therefore, incorporation of GO sheets into composites has great attention and progressively used for active packaging [1]. Although there are reports of GO or olive oil alone as a filler in the preparation of starch films [9, 21]. No research has yet been reported on the combined introduction of these two fillers within the formulation of starch network. In this study, the researchers aimed to develop and characterize starch-based films comprising olive oil and various amounts of graphene oxide plates. These composites can be hopeful environmentally friendly substances for packaging utilizations and in diverse sections of knowledge like tissue engineering.

## EXPERIMENTAL SCETION

### *Materials*

Potato starch (PS), food grade, was provided by Khoosheh Fars Starch Company (Shiraz, Iran). A commercial brand of Olive Oil (OO) was purchased from Famila CO. (Iran). Graphene Oxide (GO) was obtained from Guangzhou Feibo Co., Ltd. (Guangzhou City,

China), with thickness of .6-1.0 nm and specific surface area of 1000-1217 m<sup>2</sup>/g. Glycerol (Gly), analysis pure, was supplied from Bio Basic (Canada).

#### PS-GO film emulsion

5g of PS were dissolved in distilled water (80mL) at ambient temperature for 5min. Then the suspension exposed to steady blending (300 rpm) for 30 min at 90 °C in a water bath to complete the gelatinization process [22]. Olive oil (10% w/w based on potato starch weight) comprising Tween 80 (5% w/w based on olive oil) and glycerol (35% w/w based on potato starch weight) were combined to the potato starch solution, stirred magnetically (500 rpm, 5 min), and then made uniform with Ultraturrax (IKA T25-Digital Ultraturrax, Germany) at 13000 rpm for 4min. In the meantime, the GO powders (0, 1, 3, 5, and 9% w/w based on potato starch weight) were mixed with distilled water (20mL) under sonication in an ultrasonic (Elma, Germany) for 30 min to promote their uniform interspersion and complete exfoliation [10, 23]. Next, the GO dispersion was gradually blended to the starch emulsion, mixed magnetically for 10 min and thereupon sonicated (10 min, 100 W) up to the GO sheets were quite dispersed. Ultimately, after whole eliminated of bubbles, 23 g of the resulting mixture was strew within a polyethylene plate (diameter 9 cm) according to the ratio and placed at 40 °C for almost 24 h.

#### Water Vapor Permeability (WVP)

WVPs of polymers were determined by applying the method recommended by ASTM E96 with some modifications [17] at a constant RH of 75% at 25°C[24]. Cups with a diameter of 2 cm comprising moistureless CaCl<sub>2</sub> (0% RH) were covered with each specimen and closed with liquefied paraffin. Thereupon, the dishes were positioned in a chamber (25°C) including high-concentration solution of salt in water with RH-75%. Changing in the weight of the cup was recorded at different intervals for one week. According to the slope of the curve (namely the weight increment of the cups was registered and plotted against the time), the WVTR was computed for obtaining WVP via the following equation:

$$WVP = (WVTR \times d) / \Delta P \quad (1)$$

Where  $d$  is the film thickness (m) and  $\Delta P$  is water vapor pressure difference (Pa).

#### Moisture Content (MC) and Water Solubility (WS)

Water contents (Eq. (2)) and water solubility (Eq. (3)) were done in triplicate on the way method that recommended by Nisar *et al.*[25]. Specimens were cut (20×20 mm<sup>2</sup>) and weighed (W<sub>1</sub>). Afterwards, the sample pieces were put in curls (at 105 °C for 24h) and then weighed (W<sub>2</sub>). The solubility of films was determined by immersing them into distilled water with a steady stirring speed for 6 h at 25°C. Remaining specimen parts were separated from water applying filter. The residual sample mass was desiccate in oven at 105 °C for 24h up to a steady weight (W<sub>3</sub>). The film solubility (%) and moisture content (%) of samples was computed to Eqs. (3) and (2), respectively.

$$\text{Moisture content \%} = (W_1 - W_2) / W_1 \times 100 \quad (2)$$

$$\text{Water solubility \%} = (W_2 - W_3) / W_2 \times 100 \quad (3)$$

#### Wetting assay

The sessile drop method was utilized to evaluate the contact angle of the water droplet with the surface of the composite samples, utilizing Drop Shape Analyzer (DSA 100, KRUSS G10- Germany) at 25 ± 1°C.

#### Color properties

The color parameters of L,  $\alpha$  and b were evaluated utilizing a colorimeter (Konica Minolta Sensing, INC., Osaka, Japan), regarding the standard white plate as a reference ( $L_0^* = 97.67$ ,  $a_0^* = 0.22$ ,  $b_0^* = 0.95$ ). The total color difference ( $\Delta E$ ), Yellowness Index (YI), and Whiteness Index (WI) were calculated based on the following equations, respectively.

$$\Delta E = [(L_1^* - L_0^*)^2 + (a_1^* - a_0^*)^2 + (b_1^* - b_0^*)^2]^{0.5} \quad (4)$$

$$YI = 142.86 b^* / L^* \quad (5)$$

$$WI = 100 - [(100 - L^*)^2 + (a^*)^2 + (b^*)^2]^{0.5} \quad (6)$$

#### Ultraviolet - vis

Ultraviolet and visible light barrier characteristics of the composite specimen were quantified at selected wavelengths between 200 to 800 nm using an Ultraviolet - visible spectrophotometer (PerkinElmer, model Lambda

365, USA). Film strips were placed in a spectrophotometer test cell directly, and the air was applied as reference. The opacity value of the sample was calculated by Eq. (7).

$$\text{Opacity} = \frac{\text{Abs}_{600}}{X} \quad (7)$$

### **Mechanical testing**

To investigate mechanical properties (TS and EB), each of the samples was sliced into pieces  $10 \times 100 \text{ mm}^2$  and kept 2 days at 50% RH and  $20^\circ\text{C}$  before the test. A tensile tester (Testometric, M350-10 CT, UK) with speed of 50 mm/min and a primary grip distance of 50 mm was applied this object [24].

### **Morphological study (SEM and AFM)**

The SEM micrographs (VEGA3 Tescan, Czech Republic) at speed up voltage of 20 Kv was applied to study the morphological properties (surface and cross-sectional microscopic images) of the starch-based bio-composite films. The samples covered with a thin layer of gold with a sputter coater before analysis.

Atomic Force Microscopy (AFM) (Dualscope/Rasterscope C26, DME, Denmark) also was applied to analyze the surface topography of the specimens. Two statistical parameter including Ra and Rq were calculated utilizing a DME software (Specimen datum was converted into a 3D image).

### **Fourier-Transform InfraRed (FT-IR) spectroscopy**

To identify the possible interaction among PS/OO/GO bio-composite, the spectrophotometer of Buker Equinox 55 (Germany) was used for FT-IR analysis of composite films at the range of  $400\text{-}4000 \text{ cm}^{-1}$ .

### **Dynamic Mechanical Thermal Analysis (DMTA)**

The measurements of  $\tan\delta$  and storage modulus of composites were done by DMTA at frequency of 1 Hz, heating rate  $5^\circ\text{C}/\text{min}$ , and temperature range from  $-50$  to  $200^\circ\text{C}$ .

### **X-Ray Diffraction (XRD)**

XRD pattern was registered at 40 kV and 40 mA in the interlude of  $2\theta$  of  $5 - 50^\circ$  at a rate of  $1^\circ/\text{min}$  and a step size of  $0.02^\circ$ , using a Bruker D5000 advance diffractometer (Siemens, Germany,  $\text{Cu K}\alpha$ ).

### **Statistical analysis**

One-way analysis of variance (ANOVA) was accomplished for statistical evaluation via the SPSS statistic software (version 23.0, USA). Duncan test was employed to estimate the diverse among the specimens at the significance level of  $p < 0.05$ .

## **RESULTS AND DISCUSSIONS**

### **Water Vapor Permeability (WVP)**

Moisture sensibility of carbohydrate-based substance is a main problem in packaging applications compared to traditional plastics [21, 26]. The WVP index for control and bio-composite films was listed in Table 1. The outcomes showed that attendance of olive oil diminished the WVP amount by 31%, in comparison to the amount acquired for the net polymer. This is due to the fact that oils as nonpolar and hydrophobic materials can naturally increase the hydrophobicity of film and reduce its tendency toward water molecules [27]. Moreover, improvement in the water resistant was accomplished as a result of interactions among starch and oil water-repellent bonds [28]. These interactions cause structural changes in the starch network, leading to an increment in the twisting factor for water molecules to percolate *via* the polymer matrix, which reduces the WVP [8]. These observations are fully consistent with related work on emulsified films [8, 27]. Likewise, by combining the reinforcing filler (GO) with the emulsion film, a further significant reduction of this property can be gained (near 42%) compared with the amount obtained for the control film. The reduction of permeability could be ascribed to the excellent dispersion of GO and also this fact that the GO has more planar configuration that leads to more twist route for water vapor molecules to transmission via the starch-based composite film [10, 19]. Furthermore, the interaction between the GO sheets and the emulsion polymer network, occupy the cracks and bores in the structure of emulsion polymers (Pickering-like stabilization mechanism) [29]. In that regard, the multilayered structure of the GO plates enables them to be snared at the interface and to wind around the oil droplets and form a highly stable emulsion [13, 14]. Thus, it distributes the oil droplets evenly in the matrix polymer and prevents the oil droplets from coalescing, making the films more hydrophobic. In other word, the lipophilic

**Table 1: WVP, moisture content (MC), water solubility (WS) and contact angle ( $\theta$ ) of potato starch (PS), potato starch/olive oil (PS+10% OO) and graphene oxide-reinforced potato starch/olive oil (PS+10% OO) films**

%GO	WVP( $\times 10^{-7}$ g/m.h.Pa)	MC (%)	WS (%)	$\theta$ ( $^{\circ}$ )
0 PS	2.39 $\pm$ 2.32 <sup>a</sup>	14.90 $\pm$ 0.10 <sup>a</sup>	24.54 $\pm$ 0.21 <sup>a</sup>	41.96 $\pm$ 0.57 <sup>f</sup>
0 (PS+10%OO)	1.65 $\pm$ 1.08 <sup>b</sup>	12.31 $\pm$ 0.18 <sup>b</sup>	17.91 $\pm$ 0.39 <sup>b</sup>	44.82 $\pm$ 0.31 <sup>e</sup>
1	1.70 $\pm$ 0.59 <sup>c</sup>	12.27 $\pm$ 2.08 <sup>a</sup>	17.88 $\pm$ 4.42 <sup>b</sup>	45.91 $\pm$ 0.58 <sup>d</sup>
3	1.63 $\pm$ 1.36 <sup>ab</sup>	11.90 $\pm$ 3.90 <sup>a</sup>	17.83 $\pm$ 2.51 <sup>b</sup>	46.09 $\pm$ 0.50 <sup>c</sup>
5	1.59 $\pm$ 1.21 <sup>ab</sup>	10.85 $\pm$ 5.81 <sup>a</sup>	17.16 $\pm$ 3.33 <sup>b</sup>	53.15 $\pm$ 0.54 <sup>b</sup>
9	1.40 $\pm$ 1.04 <sup>b</sup>	9.79 $\pm$ 6.52 <sup>b</sup>	16.83 $\pm$ 5.32 <sup>b</sup>	60.34 $\pm$ 0.89 <sup>a</sup>

Values were presented as mean  $\pm$  SD. Different superscript letter in the same column indicates significant differences among formulations ( $p < 0.05$ ).

conjugated structure together with the water-absorbent -COOH and -OH groups causes GO facilely to be adsorbed at the interface of oil droplets and the starch matrix [13]. These results were according to past papers reports [7, 10].

#### Moisture Content (MC) and Water Solubility (WS)

MC (%) and WS (%) are essential features for potential commercial films [25]. The outcomes of moisture content and water solubility were showed in Table 1. By adding oil and GO into the biopolymeric matrix, MC and WS was decreased from 14.90% and 24.54% for net film to 12.31% and 17.91% for emulsion film 9.79% and 16.83% for PS-OO-GO(9%). These results indicate that the amounts of MC and WS relate to various factors like the kind of fillers and interactions in the film structure too. The FT-IR spectra provide a good evidence for the creation new H-bonds via the incorporation of oil within the biopolymeric matrices. As a result, it decrease the accessibility of -OH groups of emulsion matrix to water molecules, which in turn, leading to formation of more hydrophobicity starch-olive oil mixed [25, 30], as stated in related works [31]. Besides, the reducing effect of GO on MC and WS behaviors of starch-olive oil-graphene oxide blended films by increasing in GO content (up to 9%) were observed. This was related to the Pickering effect of GO, which it can be anchor between the starch and oil chains led to the interfacial adhesion among the GO sheets and the composite chains. This effect was stated as the vindication for reducing amounts of MC and WS of composite films due to the compact structures and reduce the inter-chain free volume of the films [32]. These conclusion was compliance with the outcomes of the previous studies [29, 33].

#### Wettability of films

The surface hydrophilicity/hydrophobicity of the samples indicate the sensitivity of the starch-based film to water or moisture [34]. The further the contact angle, the greater the lipophilic properties of the film surface (water repellency). In this regard, the emulsion film had higher contact angle (44.82 $^{\circ}$ ) rather than pure film (41.96 $^{\circ}$ ). Due to the hydrophobic nature of oils, as expected (Table 1). Similarly, *Pereda et al.*[30] studied the surface of chitosan-olive oil bio-composite films containing nanocellulose. Meantime, it is clear that GO addition further increments the contact angle of the reinforced sample with GO compare to that control films (PS and PS-OO). There was significant difference ( $p < 0.05$ ) between the contact angles of PS/OO film and the specimen comprising 9 wt. % GO (60.34 $^{\circ}$ ), which was ascribed to two general ways for reducing the wettability of composite films [35]: 1) the increased contact angle of the biocomposite samples could be ascribed to the interaction among GO and emulsion films. This result was confirmed by FTIR (Fig.2). As mentioned earlier, graphene oxide as an amphiphilic substance has hydrophobic regions [15, 36]. Therefore, when interacting with the emulsion matrix via hydrophilic regions, GO exhibited hydrophobic regions which led to poor interaction with water [37]. 2) The roughness of its surface could also affect the contact angle owing to the surface roughness of the films, causing air to be snare among the GO peaks on the films surface, creating a surface with a low sliding angle[38]. *Lyn et al.* reported the relationship between contact angle and film surface roughness [39].

#### Color coordinates and Light transmittance

The color and optical characteristic of films are a main

**Table 2: Color coordinates of potato starch (PS), potato starch/olive oil (PS+ 10% OO) and graphene oxide-reinforced potato starch/olive oil (PS+ 10% OO) films**

%GO	L*	a*	b*	ΔE	YI	WI
0 PS	93.53±0.23 <sup>a</sup>	-9.08±0.23 <sup>abc</sup>	12.77±0.49 <sup>c</sup>	15.60±0.49 <sup>d</sup>	19.15±0.73 <sup>d</sup>	83.03±0.44 <sup>a</sup>
0 (PS+10%OO)	88.74±0.24 <sup>c</sup>	-9.51±0.56 <sup>bc</sup>	14.93±0.94 <sup>b</sup>	19.23±1.01 <sup>c</sup>	24.04±1.54 <sup>c</sup>	79.01±0.98 <sup>b</sup>
1	87.77±0.22 <sup>b</sup>	-9.32±0.37 <sup>abc</sup>	15.14±0.11 <sup>b</sup>	18.09±0.11 <sup>c</sup>	29.56±0.18 <sup>c</sup>	78.40±0.10 <sup>b</sup>
3	87.32±0.46 <sup>cd</sup>	-9.88±0.46 <sup>c</sup>	18.52±0.61 <sup>a</sup>	22.32±0.64 <sup>b</sup>	31.95±0.95 <sup>b</sup>	77.95±0.61 <sup>c</sup>
5	86.10±1.26 <sup>d</sup>	-8.73±0.63 <sup>a</sup>	19.27±2.37 <sup>a</sup>	22.88±2.68 <sup>b</sup>	32.65±4.23 <sup>ab</sup>	75.29±2.68 <sup>c</sup>
9	84.74±1.00 <sup>e</sup>	-8.50±0.72 <sup>ab</sup>	20.71±0.99 <sup>bc</sup>	25.26±1.32 <sup>a</sup>	34.92±1.92 <sup>a</sup>	72.83±1.33 <sup>d</sup>

Values were presented as mean ± SD. Different superscript letter in the same column indicates significant differences among formulations (p<0.05).

feature that impacts user approval, oxidation, and their suitability as packaging materials [36, 39]. Table 2 reveal the modifications in color coordinates of different films. The net film was the lightest among all specimens. In comparison with the net sample (PS), the incorporation oil and GO resulted in decreased in lightness (L\*), meaning that the films lost clarity. Addition of oil into the PS structure caused a decline in the lightness, which this value dropped further with the GO reinforcement in the emulsion films. Redness (a\*), yellowness (b\*), Yellowness Index (YI) and total color change (ΔE) coordinates increased, but Whiteness Index (WI) decreased with augmenting GO amount in the presence of olive oil. Generally, the films blended with oil and GO sheets had brown tincture compared to pure starch film. The reason for this is the dark brown color of GO. Ahmed et al. [10] and Yang et al. [16] reported a similar color shift for CS/GO films and SA-gelatin-GO ternary composite films, respectively.

The percent transmittance (T %) of all tested samples at wavelength ambit of 200-800 nm are presented in Table 3. It is also noted that food is prone to oxidation at steep absorption in the near UV range at 200-300nm [40]. The UV transmittance dropped significantly at wavelength 200-300 nm by adding GO into the emulsion films about 100% and at 300-400 nm more than 90%. This is presumably because agglomeration of GO can cause increased light scattering and also reduced transparency in the PS-OO-GO films. The particle aggregation, which is clearly observed in the surface microscopy image in Fig. 1e, can confirm the above speculation. Absorption increased as the amount of GO in the matrix increased from 1 to 9 wt. %. As expected the film opacity ascended (data not shown). It was stated that adding the GO sheets also improved the absorption

of the samples [16, 39]. As well as, the emulsion films were more darkening (data not shown) than PS films. These results showed that the oil prevented the transmittance of ultraviolet light of the specimens, but they are not as effective as GO sheets. The same behavior has been discovered in chitosan/olive oil composites amalgamated with nanocrystals [30]. Therefore, the blended use of olive oil and GO sheets in control film can block ultraviolet rays, which may be useful to the packaging of light- susceptible materials.

#### Thickness and mechanical properties

Based on the outcome acquired from determining the thickness of starch-based samples, it was found that increasing the using of oil and GO were insignificant (p > 0.05) effect on the thickness of films. But, led to increase in specimen's thickness from 0.138 and 0.148 mm (Table 4). These results were in agreement with the previous studies on graphene oxide and PLA [10].

Tensile test result of the starch-based bio-composite films indicate their ability to withstand external effects and ductility to retain their unification under the stress exist during the processing, and storage of the packaged substances [41]. Table 4 represents the impact of GO amounts and oil on the mechanical characteristics of the samples including Tensile Strength (TS) and Elongation-at-Break (EB). Appending olive oil within the starch structure result in a significant (p<0.05) reduction in TS from 21.95 MPa to 10.57 MPa, as reported in other studies [42, 43]. It could be related to this fact that oil incompatible with the starch matrix structure forms a hydrophilic polymer, so the oil causes free volume and discontinuity in the matrix structure and also decreases the homogeneity and cohesiveness of the film matrix, resulting in poor mechanical strength [42]. Integration

**Table 3: Transmittance percentage values of Potato Starch (PS), potato starch/olive oil (PS+ 10% OO) and graphene oxide-reinforced potato starch/olive oil (PS+ 10% OO) films**

%GO	200nm T (%)	240nm T (%)	300nm T (%)	350nm T (%)	400nm T (%)	500nm T (%)	600 nm T (%)	700nm T (%)	800nm T (%)
0 PS	0.01	26.58 <sup>a</sup>	39.79 <sup>a</sup>	51.04 <sup>a</sup>	60.77 <sup>a</sup>	68.34 <sup>a</sup>	71.42 <sup>a</sup>	73.54 <sup>a</sup>	75.12 <sup>a</sup>
0 (PS+10% OO)	0.01	0.06 <sup>b</sup>	4.13 <sup>b</sup>	6.47 <sup>b</sup>	10.23 <sup>b</sup>	16.74 <sup>b</sup>	21.71 <sup>b</sup>	26.51 <sup>b</sup>	31.03 <sup>b</sup>
1	0.01	0.01 <sup>b</sup>	0.62 <sup>d</sup>	2.48 <sup>d</sup>	5.07 <sup>f</sup>	10.85 <sup>d</sup>	16.47 <sup>d</sup>	23.85 <sup>c</sup>	30.23 <sup>c</sup>
3	0.01	0.01 <sup>b</sup>	0.44 <sup>c</sup>	2.41 <sup>c</sup>	4.85 <sup>d</sup>	8.88 <sup>e</sup>	14.58 <sup>e</sup>	17.81 <sup>e</sup>	23.29 <sup>e</sup>
5	0.01	0.01 <sup>b</sup>	0.01 <sup>e</sup>	1.89 <sup>e</sup>	4.65 <sup>e</sup>	8.68 <sup>c</sup>	13.65 <sup>e</sup>	17.09 <sup>d</sup>	21.30 <sup>d</sup>
9	0.01	0.01 <sup>b</sup>	0.01 <sup>e</sup>	1.25 <sup>d</sup>	3.78 <sup>c</sup>	6.80 <sup>f</sup>	10.75 <sup>f</sup>	14.12 <sup>f</sup>	19.68 <sup>f</sup>

Mean with different letters within a column indicate significant differences ( $p < 0.05$ ).

**Table 4: Tensile properties and thickness of Potato Starch (PS), potato starch/olive oil (PS+ 10% OO) and graphene oxide-reinforced potato starch/olive oil (PS+ 10% OO) films**

%GO	Tensile strength (MPa)	Elongation-at-break (%)	Thickness (mm)
0 PS	21.95±1.18 <sup>a</sup>	10.32±0.99 <sup>a</sup>	0.138±0.01 <sup>a</sup>
0 (PS+10%OO)	10.57±0.22 <sup>b</sup>	5.34±0.42 <sup>ab</sup>	0.141±0.01 <sup>a</sup>
1	10.32±0.34 <sup>cd</sup>	5.07±2.69 <sup>b</sup>	0.142±0.01 <sup>a</sup>
3	10.96±0.20 <sup>d</sup>	4.77±0.67 <sup>b</sup>	0.146±0.01 <sup>a</sup>
5	12.13±0.80 <sup>d</sup>	4.23±0.11 <sup>ab</sup>	0.147±0.01 <sup>a</sup>
9	14.16±0.46 <sup>c</sup>	3.89±0.38 <sup>ab</sup>	0.148±0.01 <sup>a</sup>

Values were presented as mean ± SD. Different superscript letter in the same column indicates significant differences among formulations ( $p < 0.05$ ).

GO sheets with emulsion matrix increased the strength and density of the composite films, and also fortify the TS of emulsion films by increasing GO amount, as shown in Fig. 1 (f). These could be explained by fact hydrophilic groups (i.e., the ionizable edge –COOH groups) and lipophilic groups (i.e., the unoxidized graphitic patches such as phenol hydroxyl and epoxide groups) are linearly arranged (head-to-tail fashion) on the original plate of GO sheet which makes it act as a functional surfactant [44]. This structure permits the GO sheets embayed at the lipophilic/hydrophilic interfaces (Pickering effect) [45]. Therefore, interaction among GO and emulsion matrix led to preventing the bio-composite chains motion. The Pickering behavior was observed in related works on emulsions comprising GO sheet [13, 14, 44, 45]. Elongation of starch-based film a significant ( $p < 0.05$ ) decline with adding olive oil (Table 4). Similar result are reported for lower elongation of emulsion films after the addition of oil within the PS network [46–49]. Lower EB probably could be ascribed to the addition of lipophilic materials within the hydrophilic network that cause diminish the moisture amount of emulsion films. The plasticity of emulsion films was depended on their moisture amount,

since moisture acts such as a plasticizer. When the moisture amount of samples reduction result in reduce in the plasticity of the composites (EB) [50]. With the addition of GO sheets into emulsion films and raising GO amount from 1 to 9 wt. %, the elongation value was decreased. These results indicate that the chains were restricted by GO sheets.

#### Structural analysis

In order to superior comprehend the connection between the structure and performance of the starch-based bio-composite samples, the SEM images of the surface and cross-section and the AFM (3D) and the surface roughness of the composite films were showed in Fig. 1. The surface of the control sample (Fig. 1a) had the smoothest surface (roughness of 30.2 nm, Fig. 1g) and presented a continuous and homogenous structure. In addition, the cross-section image (Fig. 1b) showed a compact structure without holes or bubbles in the pure film. Similar result was also stated by *Basiak et al.* [51]. The films including oil showed a rougher surface (R: 34nm, Fig 1h) and discontinuities in the starch-base network. The SEM cross-section image (Fig.1d) of these films also indicated the difference in pore size and

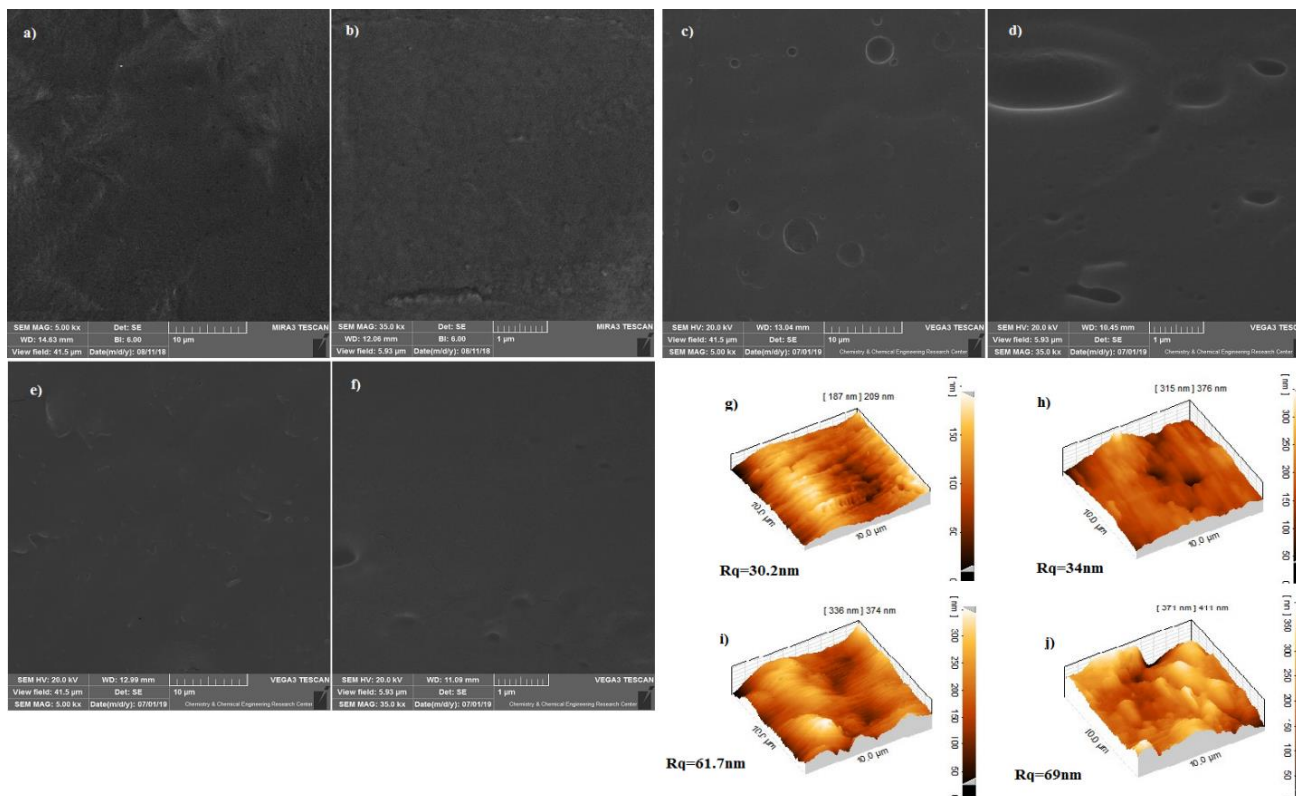


**Fig. 1:** SEM images of a) and b) starch-based films (PS), c) and d) starch-based/olive oil (10%OO) films, e) and f) PS/10%OO/graphene oxide (9% GO). AFM images and roughness (R) of surface of g) PS films, h) PS/10%OO films, i) PS/10%OO/ 3% GO and j) PS/10%OO/9%GO films ; where a, c and e demonstrates the SEM surface area and b, d and f demonstrates the SEM cross-section images

showed that the film compactness reduced. These indicate that the interaction between oil and starch matrix were flimsy [52, 53]. During drying, the oil droplets appear to be separated from the matrix film and aggregate (creaming phenomenon), leading to free spaces throughout the film and also creating irregularities at the film surface [52]. The similar behavior has been found in previously announced on the starch/oil [30, 52, 53]. The incorporation of GO (Fig. 1e) to emulsion films also affected the internal structure and film surfaces. GO (3 wt. %) sheets led to a higher surface roughness (R: 61.7nm, Fig. 1i) compared to the films prepared without using GO sheets. Meanwhile, the surface roughness of composite films increased and reached a maximum value of 69 nm (Fig. 1g) when the amount of GO was enhanced from 3 to 9 % wt. This behavior happened presumably due to the formation of agglomerates (high loading), which was caused by a possible elutriation of material to the surface during the drying process. As mentioned earlier, there is

a relationship among surface roughness and contact angle, and as the surface roughness increases, the contact angle of the films increases. This phenomenon corroborates with the results observed for hydrophobicity. A similar demeanor was also discovered by *Faradilla et al.* and *Lyn et al.* [35, 39]. Cross-section images of the composite samples comprising 9 wt. % GO (Fig. 1f) demonstrate further uniform and compact structure than the emulsion composite's structure. The uniform distribution of olive oil in the bio-composite network may also be related to the emulsification effect of GO sheets,[13, 14, 44, 45] which minimized these pores and made the films structure denser. This indicate that the prepared film was stable and ameliorated the TS and EB of the films.

#### FT-IR analysis

FT-IR tests were carried out to measure the interaction between different components, and the FT-IR spectra of olive oil, GO, pure potato starch, emulsion film and bio-composite sample based on starch loaded

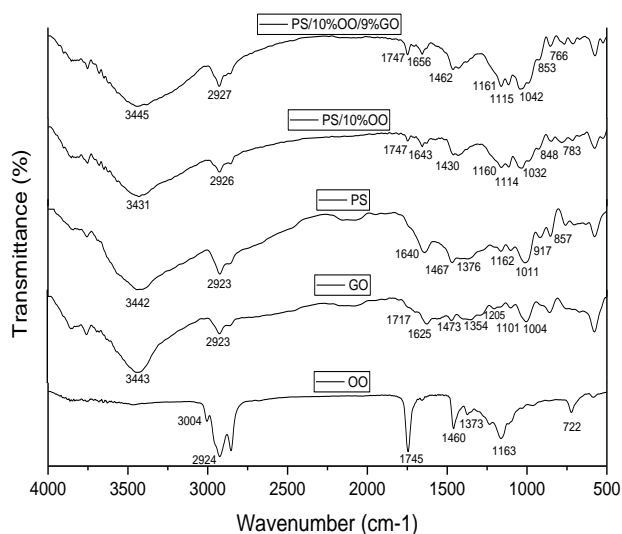


**Fig. 2:** FT-IR spectra of Olive Oil (OO), Graphene Oxide (GO), Potato Starch (PS) film, potato starch film incorporated with 10% olive oil (PS/10% OO) and potato starch/ 10% olive oil emulsion films loaded with 9% GO (PS/ 10% OO/ 9% GO)

with GO (9 wt. %) were shown in Fig.2. The FT-IR spectrum of Go showed a broad band at  $3443\text{ cm}^{-1}$ , which was related OH groups. The intense O-H band present between  $3550$  and  $3000\text{ cm}^{-1}$  gives strong indicated of intermolecular as well as intramolecular H-bonding in GO sheets [1]. The presence of peaks at  $1625\text{ cm}^{-1}$ ,  $1717\text{ cm}^{-1}$  and  $1354\text{ cm}^{-1}$  can be attributed to the stretching of C=C bond, C=O bond and the C-O of stretching bond, respectively. A small peak at  $2923\text{ cm}^{-1}$  is assigned to the stretching of C-O bond [1, 21]. For net starch film, the stretching and bending vibration of O-H groups occurred at  $3442\text{ cm}^{-1}$ ,  $1640\text{ cm}^{-1}$ , respectively. The peak at  $2923\text{ cm}^{-1}$  was characteristic of the stretching vibration of the aliphatic C-H groups. The bands at  $1467\text{ cm}^{-1}$  and  $857\text{ cm}^{-1}$  were assigned to the deformation vibrations associated with the  $\text{CH}_2$  groups. The absorptions at  $1376\text{ cm}^{-1}$  and  $1011\text{ cm}^{-1}$  can be assigned to deformation vibration of C-O-C groups. The bonds related to stretching vibration of C-O and C-C groups appear at  $1162\text{ cm}^{-1}$  and  $917\text{ cm}^{-1}$  [4, 54]. FT-IR spectrum of olive oil, the band at  $3004\text{ cm}^{-1}$  is due to the CH stretching of *cis* double bonds. The band at  $29424\text{ cm}^{-1}$  is due to the antisymmetric of aliphatic C-H in  $\text{CH}_2$  and terminal  $\text{CH}_3$  groups. The strong single peak of the C=O stretching vibration of carbonyl groups of triglycerides was observed at  $1745\text{ cm}^{-1}$ . Bands in the  $1400\text{-}1200\text{ cm}^{-1}$  region are mainly attributed

to bending vibrations of  $\text{CH}_2$  and  $\text{CH}_3$  aliphatic groups like symmetric HCH bending at  $1373\text{ cm}^{-1}$  and  $\text{CH}_2$  scissoring at  $1460\text{ cm}^{-1}$ . Peaks at  $1163\text{ cm}^{-1}$  and  $722\text{ cm}^{-1}$  correspond to the stretching vibration of C-O ester groups and overlapping of the  $(\text{CH}_2)_n$  rocking vibration and the out of-plane vibration of *cis*-di- substituted olefins [55]. By adding the olive oil within the starch network, the position of peak in the region of  $3442\text{ cm}^{-1}$ , which refers to OH groups of net starch [54] was shifted to  $3431\text{ cm}^{-1}$  in the emulsion film (10 wt. % OO). This indicates the creation of H-bonds among the starch film network and olive oil. the peak at  $1747\text{ cm}^{-1}$  corresponded to the stretching vibration of carbonyl groups of triglycerides [55, 56] of olive oil appeared in the emulsion film (10 wt. % OO), indicating the interaction between the film structure and the C=O groups of triglycerides of olive oil. By incorporating GO within emulsion composite, the position of peaks of PS at  $3442\text{ cm}^{-1}$  (OH group),  $2923\text{ cm}^{-1}$  (the C-H stretching connected with ring methane hydrogen atoms),  $1640\text{ cm}^{-1}$  (the bending vibration of -OH groups),  $1011\text{ cm}^{-1}$  (the stretching vibration of C-O in C-O-H groups) [21] shifted to higher wavenumbers of  $3445\text{ cm}^{-1}$ ,  $2927\text{ cm}^{-1}$ ,  $1656\text{ cm}^{-1}$  and  $1042\text{ cm}^{-1}$ , respectively, in the PS/10%OO/9%GO. This represents the hydrogen bond formed in the bio-composite films. Comparable findings were also realized previous papers [1, 21]. There were no new peak, which means that interactions between GO sheets and emulsion components exhibited physical interaction.

#### Dynamic Mechanical-Thermal Analysis (DMTA)

Dynamic mechanical-thermal analysis was used to study changes in phase transitions as temperature function of PS films containing olive oil and GO sheets (0, 1, 5, and 9 wt. %). Fig. 3a demonstrates the curve of  $\text{Tan } \delta$  versus temperature. As can be noticed, two relaxation processes at low (between  $-25$  and  $-18^\circ\text{C}$ ) and high ( $95^\circ\text{C}$ ) temperatures are related to the glycerol-rich domains ( $\alpha_1$  relaxation) and starch-rich domains ( $\alpha_2$  relaxation), respectively. It is worth noting that the peak of loss factor ( $\text{Tan } \delta$ ) corresponded to the  $\alpha$ - relaxation, which could be ascribed to glass transition ( $T_g$ ) [57]. Regarding Fig. 3a, the  $T_g$  temperature in both the domains declined with incorporation of oil within the potato starch structure, which was ascribed to the lubrication theory. In fact, oils behave like lubricants

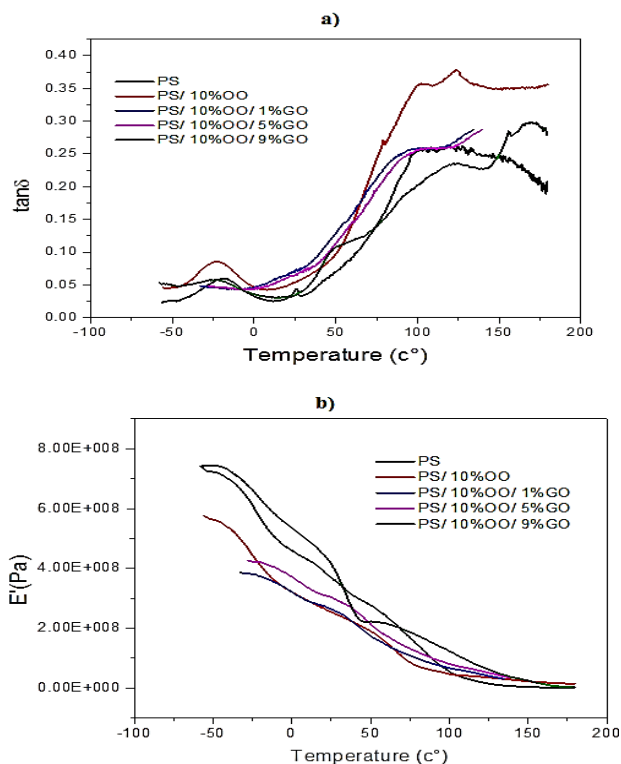


**Fig. 3:** DMTA curve: (a) Loss factor ( $\tan\delta$ ) and (b) Storage modulus of control film, potato starch film incorporated with 10% olive oil and potato starch/ 10% olive oil emulsion films loaded with different amounts of GO

and alleviate the friction force among the chains of polymer and enhance the vacant space, makes decreased  $T_g$  of emulsion composite [46]. With the addition of GO at distinct amounts in the starch-oil network, the situation of both temperature relaxations (i.e. glass transition temperature of glycerol- ( $T_{gGRP}$ ) and starch-rich ( $T_{gSRP}$ ) domains) enhanced. As shown, the influence of GO sheets on the position of  $T_{gSRP}$  is more significant than the position of  $T_{gGRP}$ , notably with the increase in the GO content. Thus, it can be mentioned that the presence of GO in emulsion matrices simplifies the interaction of PS with oils and diminishes the phase dissociation event and also the free space inside the film structure, consequently, hinders the chain movement. Additionally, GO is dispersed well in the emulsion matrix. As expected, oils indicate lubrication effect and caused to diminish in the toughness of emulsion structure, leading to a decrease the storage modulus of sample (Fig. 3b). It is clear that by loading GO over 1 wt. % the storage modulus of film decreased. These may be due to the reduction in the quantity of GO

participating in oil-GO sheets interactions, so in low amounts GO cannot act as reinforcement. Thereby, at very low amount, it functions highly probably as an imperfection rather than as a reinforcement. By adding higher GO contents (up to 5 wt. %) compared to emulsion film no increase was observed in storage modulus. This demeanor is obvious in the down temperature range (i.e. -40 to -10°C). However, at upper temperatures (i.e. -10 to 180°C), the storage modulus increased. Presumably because GO (5 wt. %) did not show the expected reinforcing effect at low temperatures. By further increasing the GO content up to 9 wt.%, fiber aggregation becomes more apparent, as a result a considerable increase in the composite storage modulus and even greater than the corresponding unreinforced system (PS film). However, in this case, the dependence of the storage module on the GO amount (from 1 to 9 wt. %) is obvious.

#### XRD analysis

The results of XRD characterization of PS, PS/10%OIL and PS/10%OIL/GO-n films were displayed in Fig. 4. As known, starch has a semi-crystalline nature and the crystal structure of starch can be classified in 3 forms (A, B and C) [4]. The net starch film (PS) had a B-type crystalline pattern (usually found in tuber starch like a potato), which appeared four main reflections at about 5.4°, 17.1°, 19.8°, and 22.3° [21]. The GO pattern revealed a high and narrow crystallization peak near 10.87° and also according Bragg equation the d-spacing was 8.1Å. Similarly, such a result has previously stated by other researchers [58, 59]. After integrating with olive oil (PS/10%OIL), the two diffraction peaks disappeared at 5.4° and 22.3°, and also the intensity of the peak at 17.1° was remarkably reduced in contrast to the control film. It is speculated the inclusion of oil has a destructive effect on the crystallinity of the emulsion network. This occurrence corresponded to the new interactions among starch and olive oil (namely the hydrophobic interactions among the C=O group of the fatty acids and the OH groups of starch), which forms a large complex that prevents the reorganization of potato starch chains [42]. In other words, the new inactions between oil and starch destroy the original crystalline structure of the starch. These new interactions were confirmed by FT-IR spectroscopy;

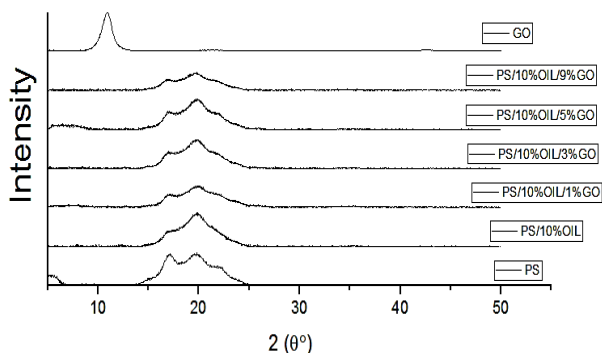


**Fig. 4:** XRD patterns of graphene oxide (GO), potato starch (PS) film, potato starch film incorporated with 10% olive oil (PS/10% OO) and potato starch/ 10% olive oil emulsion films loaded with different amounts of GO

as reported in related works when different degrees of unsaturation fatty acid were added into the sweet potato starch-based films [43]. With adding GO to the emulsion film (PS/10%OIL/GO-n) the reflections for these peaks gradually reduced. The decrease of peak intensity presumably could be owing to were superb exfoliated and uniformly interspersed of GO in the emulsion structure, leading to increments number of H-bonds and the reduce of regular domains, thus led to notable slowing down of potato starch re-crystallization [1, 21]. The similar trend has been found in the GO-PVA composite films [1] and the SA-gelatin-GO composite films [16]. Hence, the XRD spectrum of the GO sheets disappeared in the starch-base bio-composite films.

## CONCLUSIONS

This study is aimed the development of a bio-composite film made from an inexpensive source of polysaccharide (starch), incorporated with olive oil and GO using the solution casting method. The WVP, moisture content and solubility results demonstrated that percolation of moisture can be considerably decreased by the incorporation of GO and oil. However, applying oil and GO increased the surface hydrophobicity of the bio-composite films. The results from UV light shown strong UV -protection, notably the PS/10%OIL/9%GO film. The use of oil and GO in the network of the polymers debilitated and strengthened their mechanical properties, respectively. The XRD pattern showed exfoliation of the GO sheets and the FT-IR spectra demonstrated formation of the physical bonds (hydrogen bonding) between GO, oil and biopolymer. The

improvement and deterioration of thermal stability of composite films by adding GO sheets and oil into the film matrix by DMTA result were confirmed, respectively. SEM and AFM micrographs were proved GO sheets were well compatible with the film system and also showed the evenness of films without presence of holes or fractures. In summary, the bio-composites films with improved performance were produced from inexpensive and green materials. As well as can also be contemplated as a prospective packaging substance for moisture resistance and UV-proof.

## Acknowledgments

The authors wish to express their gratitude to Tehran University and Iran Polymer and Petrochemical Institute for their technical support.

Received : Dec.06, 2022 ; Accepted : Mar.06, 2023

## REFERENCES

- [1] Usman A., Hussain Z, Riaz A ., Khan A N., [Enhanced Mechanical, Thermal and Antimicrobial Properties of Poly \(Vinyl Alcohol\)/Graphene Oxide/Starch/Silver Nanocomposites Films](#), *Carbohydr Polym.*, **153**: 592–599 (2016).
- [2] Khanzadi M., Jafari S.M., Mirzaei H., Chegini FK., Maghsoudlou Y., Dehnad D., [Physical and Mechanical Properties in Biodegradable Films of Whey Protein Concentrate-Pullulan by Application of Beeswax](#), *Carbohydr Polym.*, **118**: 24–29 (2015).
- [3] Vahedikia N., Garavand F., Tajeddin B., Cacciott I., Jafari S.M., Omidi T., Zahedi Z., [Biodegradable Zein Film Composites Reinforced with Chitosan Nanoparticles and Cinnamon Essential Oil: Physical, Mechanical, Structural and Antimicrobial Attributes](#), *Colloids Surfaces B Biointerfaces*, **177**: 25–32 (2019).
- [4] Popescu M.C., Dogaru B.I., Goanta M., Timpu D., [Structural and Morphological Evaluation of CNC Reinforced PVA/Starch Biodegradable Films](#), *Int J Biol Macromol*, **116**: 385–393 (2018).
- [5] Jiménez A., Fabra M.J., Talens P., Chiralt A., Jiménez A., Fabra M.J., Talens P., Chiralt A., [Physical Properties and Antioxidant Capacity of Starch-Sodium Caseinate Films Containing Lipids](#), *J Food Eng*, **116**: 695–702 (2013).

- [6] Ge X., Li H., Wu L., Li P., Mu X., Jiang Y.J., [Improved Mechanical and Barrier Properties of Starch Film with Reduced Graphene Oxide Modified by SDBS](#), *Appl Polym Sci.*, **134**: 44910 (2017).
- [7] Wu Z., Huang Y., Xiao L., Lin D., Yang Y.Y., Wang H., Wu D., Chen H., Zhang Q., Qin W., Pu, S., [Physical Properties and Structural Characterization of Starch/Polyvinyl Alcohol/Graphene Oxide Composite Films](#), *J. Ijbioma.*, **123**: 569–575 (2019).
- [8] Acosta S., Jiménez A., Cháfer M., González- Martínez C., Chiralt A., [Physical Properties and Stability of Starch-Gelatin Based Films as Affected by the Addition of Esters of Fatty Acids](#), *Food Hydrocoll.*, **49**: 135–143 (2015).
- [9] Jeevahan J., Chandrasekaran M., [Effect of Olive oil Concentrations on Film Properties of Edible Composite Films Prepared from Corn starch and Olive Oil](#), *J. Pharm. Technol.*, **11**: 4934–4938 (2018).
- [10] Arfat Y A., Ahmed J., Ejaz M., Mullah M., [Poly lactide/Graphene Oxide Nanosheets/Clove Essential Oil Composite Films for Potential Food Packaging Applications](#), *Int. J. Biol. Macromol.*, **107**: 194-203 (2018).
- [11] Slavutsky A.M., Bertuzzi M.A., [Water Barrier Properties of Starch Films Reinforced with Cellulose Nanocrystals Obtained from Sugarcane Bagasse](#), *Carbohydr Polym.*, **110**: 53-61 (2014).
- [12] Zhu Y., Murali S., Cai W., Li X., Suk J.W., Potts J.R., Ruoff R.S., [Graphene and Graphene Oxide: Synthesis, Properties, and Applications](#), *Adv. Mater.*, **22**: 3906–3924 (2010).
- [13] Chen X., Song X., Huang J., Wu C., Ma D., Tian M., Jiang, H., Huang P., [Phase Behavior of Pickering Emulsions Stabilized by Graphene Oxide Sheets and Resins](#), *Energy & Fuels.*, **31**: 13439- 13447 (2017).
- [14] He Y., Wu F., Sun X., Li R., Guo Y., Li C., [Factors that Affect Pickering Emulsions Stabilized by Graphene Oxide](#), *J ACS Appl. Mater. Interface.*, **5**: 4843–4855 (2013).
- [15] Cote L.J., Kim J., Tung V.C., Luo J., Kim F., Huang J., [Graphene Oxide as Surfactant Sheets](#), *Pure. Appl. Chem.*, **83**: 95-110 (2010).
- [16] Yang L., Yang J., Qin X., Kan J., Zeng F., Zhong J., [Ternary Composite Films with Simultaneously Enhanced Strength and Ductility: Effects of Sodium Alginate-Gelatin Weight Ratio and Graphene Oxide Content](#), *Int. J. Biol. Macromol.*, **156**: 494–503 (2020).
- [17] Ma T., Chang P.R., Zheng P., Ma X., [The Composites Based on Plasticized Starch and Graphene Oxide/Reduced Graphene Oxide](#), *Carbohydr Polym.*, **94**: 63-70 (2013).
- [18] Sharma B., Shekhar S., Gautam S., Jain P., [Dynamic Shear Rheology Behavior and Long Term Stability Kinetics of Reduced Graphene Oxide Filled Poly \(Vinyl Alcohol\) Biofilm](#), *Polym. Test.*, **69**: 583-592 (2018).
- [19] Ahmed J., Mulla M., Arfat Y.A., [Mechanical, Thermal, Structural and Barrier Properties of Crab Shell Chitosan/Graphene Oxide Composite Films](#), *Food Hydrocoll.*, **71**: 141-148 (2017).
- [20] Najafabadi S.A.A., Mohammadi A., Kharazi A.Z., [Polyurethane Nanocomposite Impregnated with Chitosan-Modified Graphene Oxide as a Potential Antibacterial Wound Dressing](#), *Mater. Sci. Eng. C.*, **115**: 110899 (2020).
- [21] Li R., Liu C., Ma J., [Studies on the Properties of Graphene Oxide-Reinforced Starch Biocomposites](#), *Carbohydr Polym.*, **84**: 631-637 (2011).
- [22] Almasi H., Ghanbarzadeh B., Entezami A.A., [Physicochemical Properties of Starch-CMC-Nanoclay Biodegradable Films](#), *Int. J. Biol. Macromol.*, **46**: 1-5 (2010).
- [23] Dai H., Huang Y., Huang H., [Eco-Friendly Polyvinyl Alcohol/Carboxymethyl Cellulose Hydrogels Reinforced with Graphene Oxide and Bentonite for Enhanced Adsorption of Methylene Blue](#), *Carbohydr. Polym.* **185**: 1-11 (2018).
- [24] Zhang S., Zhao H., [Preparation and Properties of Zein-Rutin Composite Nanoparticle/Corn Starch Films](#), *Carbohydr. Polym.*, **169**: 385-392 (2017).
- [25] Nisar T., Wang Z.C., Yang X., Tian Y., Iqbal M., Guo Y., [Characterization of Citrus Pectin Films Integrated with Clove Bud Essential Oil: Physical, Thermal, Barrier, Antioxidant and Antibacterial Properties](#), *Int. J. Biol Macromol.*, **106**: 670-680 (2018).
- [26] Bahrami A., Mokarram R.R., Khiabani M.S., Ghanbarzadeh B., Salehi R., [Physico-Mechanical and Antimicrobial Properties of Tragacanth/Hydroxypropyl Methylcellulose/Beeswax Edible Films Reinforced with Silver Nanoparticles](#), *Int. J. Biol. Macromol.*, **129**: 1103-1112 (2019).
- [27] Xiao J., Wang W., Wang K., Liu Y., Liu A., Zhang S., [Impact of Melting Point of Palm Oil on Mechanical and Water Barrier Properties of Gelatin-Palm oil Emulsion Film](#), *Food Hydrocoll.*, **60**: 243-251 (2016).

- [28] Gutiérrez T.J., Tapia M.S., Pérez E., Famá L., [Edible Films Based on Native and Phosphated 80: 20 Waxy: Normal Corn Starch](#), *Starch Stärke.*, **67**: 90-97 (2015).
- [29] Li K., Jin S., Li J., Chen H., [Improvement in Antibacterial and Functional Properties of Mussel-Inspired Cellulose Nanofibrils/Gelatin Nanocomposites Incorporated with Graphene Oxide for Active Packaging](#), *Ind. Crops. Prod.*, **132**: 197-212 (2019).
- [30] Pereda M., Dufresne A., Aranguren M.I., Marcovich N.E., [Polyelectrolyte Films Based on Chitosan/Olive Oil and Reinforced with Cellulose Nanocrystals](#), *Carbohydr. Polym.*, **101**: 1018-1026 (2014).
- [31] Vargas M., Albors A., Chiralt A., González-Martínez C., [Characterization of Chitosan-Oleic Acid Composite Films](#), *Food Hydrocoll.*, **23**: 536-547 (2009).
- [32] Hosseini S.F., Rezaei M., Zandi M., Farahmandghavi F., [Fabrication of Bio-Nanocomposite Films Based on Fish Gelatin Reinforced with Chitosan Nanoparticles](#), *Food Hydrocoll.*, **44**: 172-182 (2015).
- [33] Afshar S., Baniasadi H., [Investigation the Effect of Graphene Oxide and Gelatin/Starch Weight Ratio on the Properties of Starch/Gelatin/GO Nanocomposite Films: The RSM Study](#), *Int. J. Biol. Macromol.*, **109**: 1019 (2018).
- [34] Kokoszka S., Debeaufort F., Lenart A., Voilley A., [Water Vapour Permeability, Thermal and Wetting Properties of Whey Protein Isolate Based Edible Films](#), *Int. Dairy. J.*, **20**: 53-60 (2010).
- [35] Faradilla R.H.F., Lee G., Roberts J., Martens P., Stenzel M., Arcot J., [Effect of Glycerol, Nanoclay and Graphene Oxide on Physicochemical Properties of Biodegradable Nanocellulose Plastic Sourced from Banana Pseudo-Stem](#), *Cellulose.*, **25**: 399-416(2018).
- [36] Yan J W., Hu C., Chen K., Lin Q.B., [Release of Graphene from Graphene-Polyethylene Composite Films into Food Simulants](#), *Food Package Shelf Life.*, **20**: 100310 (2019).
- [37] Gao L., Zhu T., He F., Ou Z., Xu J., Ren L., [Preparation and Characterization of Functional Films Based on Chitosan and Corn Starch Incorporated Tea Polyphenols](#), *Coatings.*, **11**: 35-41 (2021).
- [38] Miwa M., Nakajima A., Fujishima A., Hashimoto K., Watanabe T., [Effects of the surface roughness on sliding angles of water droplets on superhydrophobic surfaces](#), *Langmuir* **16**: 5754-5760 (2000).
- [39] Lyn F.H., Peng T.C., Ruzniza M.Z., Hanani Z.A.N., [Effect of Oxidation Degrees of Graphene Oxide \(GO\) on the Structure and Physical Properties of Chitosan/GO Composite Films](#), *Food Package Shelf Life.*, **21**: 100373 (2019).
- [40] Rouhi J., Mahmud S., Naderi N., Ooi C.H.R., Mahmood M.R., [Physical Properties of Fish Gelatin-Based bio-Nanocomposite Films Incorporated with ZnO Nanorods](#), *Nanoscale Res. Lett.*, **8**: 1-8 (2013).
- [41] Zhou X., Zong X., Wang S., Yin C., Gao X., Xiong G., Xu X., Qi J., Mei L., [Emulsified Blend Film Based on Konjac Glucomannan/Carrageenan/ Camellia Oil: Physical, Structural, and Water Barrier Properties](#), *Carbohydr Polym.*, **251**: 117100 (2021).
- [42] Giannakas A., Patsoura A., Barkoula N.M., Ladavos A., [A Novel Solution Blending Method for Using Olive Oil and Corn Oil as Plasticizers in Chitosan Based Organoclay Nanocomposites](#), *Carbohydr Polym.*, **157**: 550-557 (2017).
- [43] Liu P., Sun S., Hou H., Dong H., [Effects of Fatty Acids with Different Degree of Unsaturation on Properties of Sweet Potato Starch-Based Films](#), *Food Hydrocoll.*, **61**: 351-357 (2016).
- [44] Kim J., Cote L.J., Kim F., Yuan W., Shull K.R., Huang J.J., [Graphene Oxide:Surface Activity and Two Dimensional Assembly](#), *Am Chem Soc.*, **22**:1954-1958 (2010).
- [45] Pickering S.U., [Cxcvi.-Emulsions](#), *J. Chem. Soc. Trans.*, **91**: 2001-2021 (1907).
- [46] Ghanbarzadeh B., Almasi H., Zahedi Y., ["Biodegradable Edible Biopolymers in Food and Drug Packaging"](#), Amir Kabir University of Technology, Tehran (2009).
- [47] Guerrero P., Hanani Z.A.N., Kerry J.P., De La Caba K., [Characterization of Soy Protein-Based Films Prepared with Acids and Oils by Compression](#), *J. Food Eng.*, **107**: 41-49 (2011).
- [48] Péroval C., Debeaufort F.F., Despré D., Voilley A.A.A., [Edible Arabinoxylan-Based Films. 1. Effects of Lipid Type on Water Vapor Permeability, Film Structure, and Other Physical Characteristics](#), *J. Agric Food Chem.*, **50**: 3977-3983 (2002).
- [49] Valenzuela C., Abugoch L., Tapia C., [Quinoa Protein-Chitosan-Sunflower Oil Edible Film: Mechanical, Barrier and Structural Properties](#), *LWT-Food Sci. Technol.*, **50**: 531-537 (2013).

- [50] Lee M.H., Kim S.Y., Park H., [Effect of Halloysite Nanoclay on the Physical, Mechanical, and Antioxidant Properties of Chitosan Films Incorporated with Clove Essential Oil](#), *J. Food Hydrocoll.*, **84**: 58-67 (2018).
- [51] Basiak E., Lenart A., Debeaufort F., [Effect of Starch Type on the Physico-Chemical Properties of Edible Films](#), *Int. J. Biol. Macromol.*, **98**: 348-356 (2017).
- [52] Galus S., Kadzińska J., Kadzińska J., [Whey Protein Edible Films Modified with Almond and Walnut Oils](#), *J. Food Technol. Biotechnol.*, **54**: 78-86 (2016).
- [53] Kadzińska J., Bryś J., Ostrowska-Ligęza E., Estéve M., Janowicz M., [Influence of Vegetable Oils Addition on the Selected Physical Properties of Apple–Sodium Alginate Edible Films](#), *Polym. Bull.*, **77**: 88-900 (2020).
- [54] Wu Y., Geng F., Chang P.R., Yu J., Ma X., [Effect of Agar on the Microstructure and Performance of Potato Starch Film](#), *Carbohydr Polym.*, **76**: 299-304 (2009).
- [55] de la Mata P., Dominguez-Vidal A., Bosque-Sendra J.M., Ruiz-Medina A., Cuadros-Rodríguez L., Ayora-Cañada M.J., [Olive Oil Assessment in Edible Oil Blends by Means of ATR-FTIR and Chemometrics](#), *Food Control.*, **23**: 449-455 (2012).
- [56] Uncu O., Ozen B., Tokatli F., [Use of FTIR and UV-Visible Spectroscopy in Determination of Chemical Characteristics of Olive Oils](#), *Talanta.*, **201**: 65-73 (2019).
- [57] Zhang H.Y., Tehrany E.A., Kahn C.J.F., Ponçot M., Linder M., Cleymand F., [Effects of Nanoliposomes Based on Soya, Rapeseed and Fish Lecithins on Chitosan thin Films Designed for Tissue Engineering](#), *Carbohydr Polym.*, **88**: 618–627 (2012).
- [58] Ionita M., Pandeale M.A., Iovu H., [Sodium Alginate/Graphene Oxide Composite Films with Enhanced Thermal and Mechanical Properties](#), *Carbohydr Polym.*, **94**: 339-34(2013).
- [59] Wang J., Wang X., Xu C., Zhang M., Shang X., [Preparation of Graphene/Poly \(Vinyl Alcohol\) Nanocomposites with Enhanced Mechanical Properties and Water Resistance](#), *Polym. Int.*, **60**: 816-822 (2011).